17th World Conference on Earthquake Engineering, 17WCEE
Sendai, Japan - September 13th to 18th 2020

INVESTIGATION FOR SUBSIDENCE AT THE APPROACHING AREAS OF ABUTMENTS INDUCED BY SEQUENCED GROUND MOTIONS

Y. Kajita[(1)], S. Fukui[(2)], T. Kitahara[(3)], K. Uno[(4)], T. Mazda[(5)]

[(1)] *Associate Professor, Dept. of Civil and Structural Eng., Kyushu University, ykajita@doc.kyushu-u.ac.jp*
[(2)] *Graduate Student, Dept. of Civil and Structural Eng., Kyushu University, fukui@doc.kyushu-u.ac.jp*
[(3)] *Professor, Department of Science and Engineering, Kanto Gakuin University, kitahara@kanto-gakuin.ac.jp*
[(4)] *Manager, Institute of Technology, Penta-Ocean Construction Co. Ltd., kunihiko.uno@mail.penta-ocean.co.jp*
[(5)] *Professor, Dept. of Civil and Structural Eng., Kyushu University, mazda@doc.kyushu-u.ac.jp*

Abstract

In the 2016 Kumamoto earthquake, the activities of two different fault zones were performed in a short period of time. Japanese seismic intensity of 6 lower, which is considered to be equivalent to the current design ground motion, was observed in Mashiki town five times in about 28 hours. In general, when we design a bridge, only one exposure to strong ground motion is considered. Therefore, if there is a possibility that multiple strong ground motions may act to a bridge and if there is a possibility that the damage to the structure expands in a short period of time, it becomes a big problem how to prescribe the required performance such as seismic safety, serviceability and repairability for bridges.

Based on the damage of the 2011 off the Pacific coast of Tohoku Earthquake, the authors have conducted two-dimensional effective stress analysis considering the interaction between the ground and the bridge which crosses a river. We have been studying the damage control effect of the approaching area of the abutment by the ground improved methods. In the past study, the severe ground motion was inputted at one time.

In this study, we focused on the subsidence phenomenon of the approaching area of the abutment when two strong motions, the foreshock on April 14, 2016 and the main shock on April 16, 2016, were input to a virtual bridge across the river. So, the purpose of this study is to confirm the vertical gap of the abutment and the curvature of pile induced by repeated earthquake motions. Seismic response analysis is performed for three cases. One is a model inputting fore shock only. Another is a model inputting main shock only. The other is the model inputting fore shock and main shock continuously. As a result, the final vertical gap is almost same even if the occurrence order of two seismic motion is changed. And the vertical gap of the model inputting fore shock and main shock continuously is smaller than the sum of the result of the model inputting fore shock and the model inputting main shock. The maximum curvature of the pile in the case that the foreshock and main shock are input consecutively is larger than the case of only the main shock. Same as the vertical gap, the maximum horizontal displacement of the pile is almost same even if the occurrence order of two seismic motion is changed.

Keywords: sequenced ground motions, liquefaction, abutment, subsidence of the backfill soil

1. Introduction

The subsidence of the soil at the approaching area of the abutment and the horizontal movement of the abutment were observed in the 2011 off the Pacific Coast of Tohoku earthquake and the 2016 Kumamoto earthquake. This is because the lateral flow was generated in the soft ground due to the severe ground excitation [1, 2]. If the amount of the subsidence was large, the emergency cars would not be able to pass through the bridge just after a severe earthquake. In the 2016 Kumamoto Earthquake, steps on the approach section behind abutment were reported on many bridges across rivers, and it was also confirmed that the steps on the backside of the abutment were enlarged by multiple earthquake motions as shown in Photo 1. The purpose of this study is to confirm the vertical gap of the abutment and the curvature of pile induced by repeated earthquake motions. In this analysis, we also focused on the occurrence order of the sequenced seismic motions.

(a)photo taken on April 14

(b)photo taken on May 13

Photo 1 - Enlargement of damage

2. THE OUTLINE OF TWO DIMENSIONAL EFFECTIVE STRESS ANALYSIS

2.1 The modelling of structures and ground

In this analysis, FLIP, Finite element analysis program of liquefaction process/response of soil-structure systems during earthquake, which is a dynamic effective stress analysis program is used [3,4]. Fig. 1 shows the numerical model in this analysis, and the locations of the front ground and the back ground described later are shown in Figure 1. The girder (orange line) is connected to the pier rigidly. The clearance between the girder and the abutment is set to be 10cm. The ground consists of 5 layer types. The physical properties of each layer is shown in Table 1. In Table 1, Layer1 and Layer 2 are the ground at the back of the abutment. Layer3 is the ground just under the foundation of the abutments and the pier. In this analysis, it is assumed that only Layer3 is a liquefaction layer. So the excess pore water pressure ratio at the Layer3 is calculated. The excess pore water pressure ratio is defined the ratio of the excess pore water pressure to the initial effective mean stress. This analysis is conducted under the drained condition and the coefficient of permeability is set to be 1.0E-4 m/s in this analysis. The moment-curvature relationship of the piles is defined as the bi-linear model as shown in Fig. 2. The foundation piles are steel tube piles whose diameter is 800mm, and thickness is 12mm. The foundation piles are arranged three in the bridge-axial direction, four in the orthogonal direction. The foundation piles of the abutment and the ones of the pier is same material and size. The bottom of the numerical model in Fig. 1 is the surface of the engineering base. In this model, the

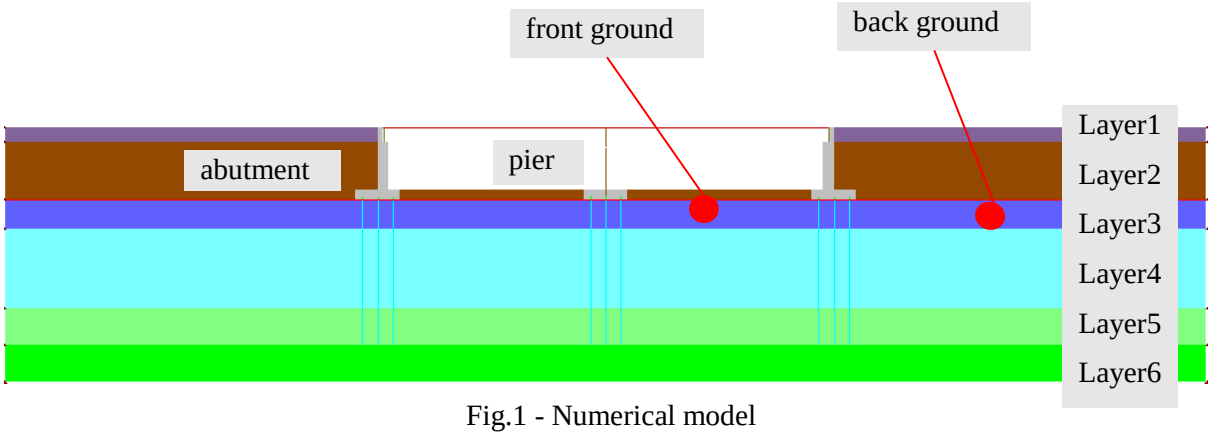

Fig.1 - Numerical model

Table 1 - The physical properties of each layer

	N-value	Thickness of a layer (m)	Density (t/m^3)	Internal friction angle (degree)	Average effective restraint pressure (kPa)
layer1	5	2.1	1.92	38.3	15.44
layer2	10	7.9	1.92	36.9	88.94
layer3	2	5.0	1.92	30.0	183.75
layer4	10	10.0	1.92	33.4	301.35
layer5	20	5.0	1.92	36.3	418.95
layer6	50	5.0	1.92	41.7	492.45

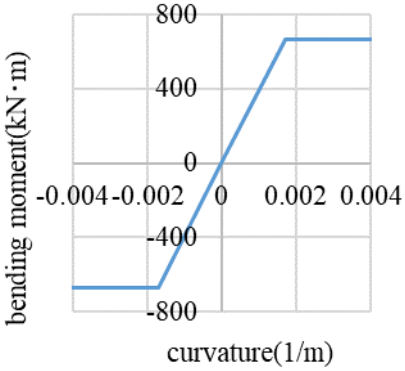

Fig.2 - Moment-curvature relationship of steel pile

node of the end member for steel pile is located at the bottom of the numerical model. That means the movement of the end member for steel pile is same as the movement of the engineering base surface.

2.2 Input earthquake motion at the engineering base

Firstly, two ground surface motions, which are the observation records in the foreshock and the main shock of the 2016 Kumamoto Earthquake, are prepared. These records are the ground surface acceleration of the East-West direction recorded in Mashiki-town, Kumamoto Prefecture. The observation point is KMMH016 by Strong-motion seismograph networks in Japan [5]. In this analysis, the acceleration at the engineering base is needed. So, the acceleration at the engineering base is calculated by using one-dimensional wave propagation analysis. Fig. 3 shows the input waves at the engineering base. The maximum acceleration of the foreshock and the main shock are 563 cm/s^2 and 658cm/s^2, respectively.

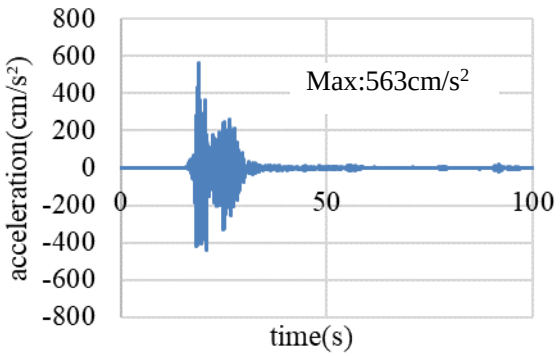

(a) foreshock motion

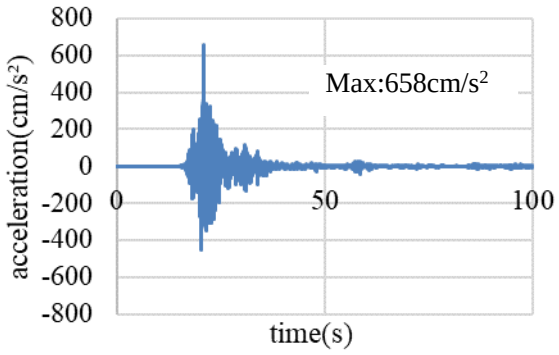

(b) main shock motion

Fig.3 - Input seismic acceleration at engineering base

2.3 Analytical cases

Seismic response analysis is performed for three cases. One is a model inputting the foreshock wave only. Another is a model inputting the main shock only. The other is the model inputting fore shock and main shock continuously. In this research, we focus on the occurrence order of the two shocks. So, the numerical analyses are conducted both the case where the foreshock is inputted and then the main shock is inputted and the case where the main shock is inputted and then the foreshock is inputted. As I mentioned before, in this analysis, the drain condition is adopted. The time interval between these two shocks is set to be 2500 sec in this analysis. We checked the excess pore water pressure keeps constant after 2500 seconds in advance.

3. ANALYTICAL RESULTS AND DISCUSSIONS

3.1 The ratio of excess pore water pressure and the amount of vertical gap

Time history of the excess pore water pressure ratio recorded in the front ground and the back ground are shown in Fig. 4. The location of the front ground and the back ground is shown in Fig. 1. The time history of excess pore water pressure ratio during the excitation is also shown in Fig. 5. It can be seen that the excess pore water pressure ratio at the front ground is larger than the one at the back ground. The excess pore water pressure ratio is defined as the ratio between excess pore water pressure created by repeated shearing and the original effective overburden pressure. The effective overburden pressure at the back ground is much larger than the one at the front ground, so the excess pore water pressure ratio at the back ground is smaller. It is found from Fig. 4 and Fig. 5 that the excess pore water pressure ratio experienced a sharp rise during the peak of seismic motion and then the excess pore water pressure ratio also experienced a gradual decrease post-peak. After the convergence of the excess pore water pressure ratio, the second seismic wave inputted, then, the excess pore water pressure ratio increased again. But the peak value did not exceed the peak value for the first seismic motion even if the occurance order of the seismic waves was changed. This could be attributed to the fact that the ground experienced compaction during the first seismic motion, thus preventing notable liquefaction.

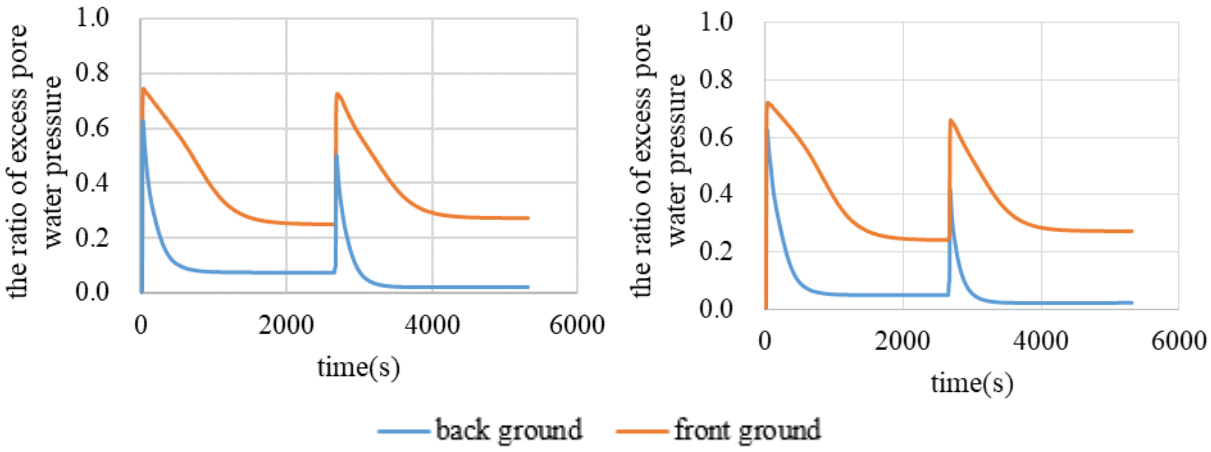

(a) main shock after foreshock (b)foreshock after main shock

Fig.4 - Time history of the ratio of excess pore water pressure

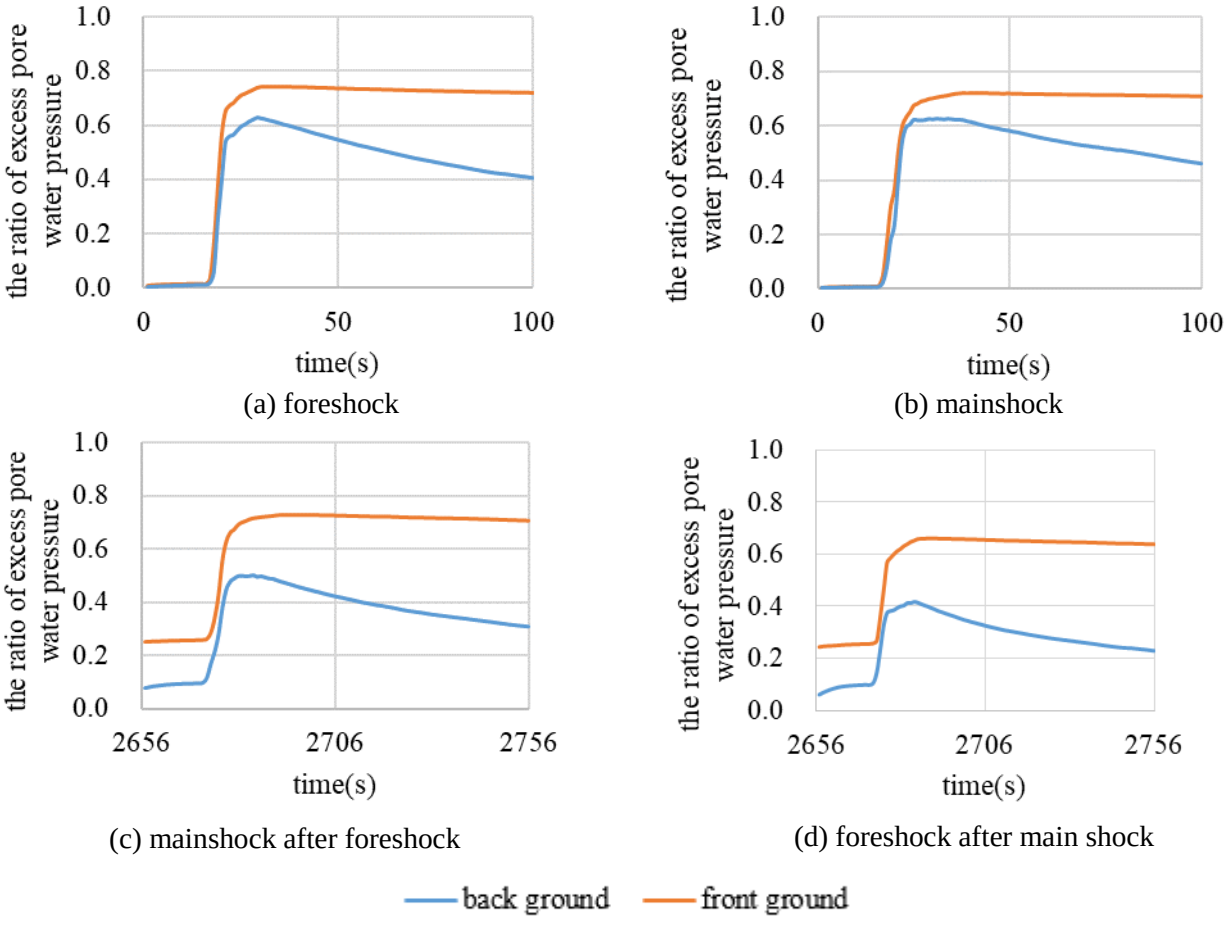

(a) foreshock (b) mainshock

(c) mainshock after foreshock (d) foreshock after main shock

Fig.5 - Time history of the amount of excess pore water pressure during vibration

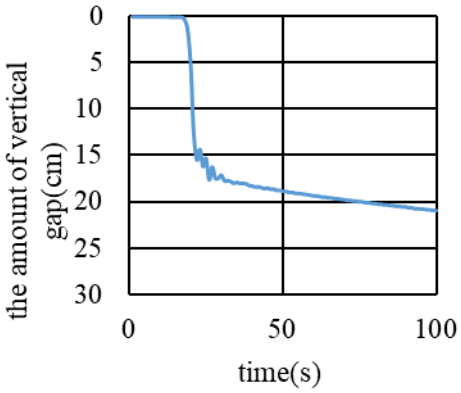

(a) foreshock

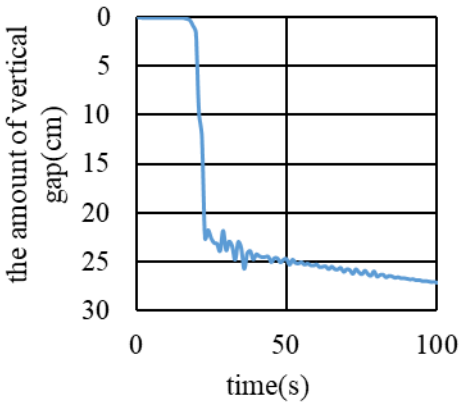

(b) mainshock

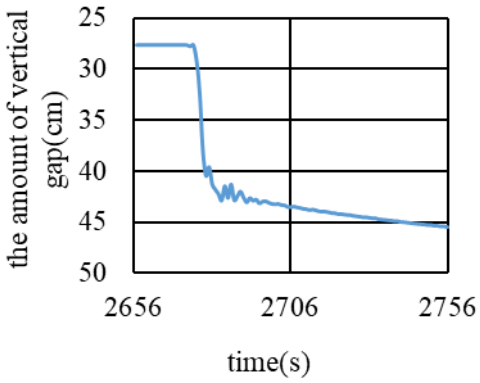

(c) mainshock after foreshock

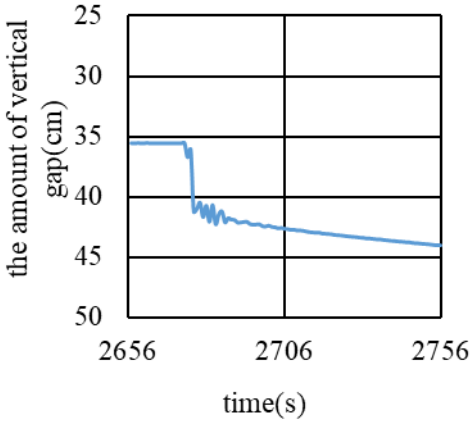

(d) foreshock after main shock

Fig.6 - Time history of the amount of vertical gap during vibration

Fig. 6 shows the time history of the amount of vertical gap on the right side during the vibration. The vertical gap is defined as the vertical difference between the top of the abutment and the backfill soil. From Fig. 5 and Fig. 6, it can be confirmed that the time when the vertical step increases is coincide with the time when the excess pore water pressure ratio increases.

Fig. 7 shows the time histories of the amount of vertical gap in each case. After the start of the vibration, the amount of vertical gap increased rapidly in the time of the peak earthquake motion, and then gradually increased with the drainage. The drainage was almost completed and there was almost no change in the level difference, and the graph also confirmed that the time when the size of the level difference converged and the time when the excess pore water pressure ratio converged coincided.

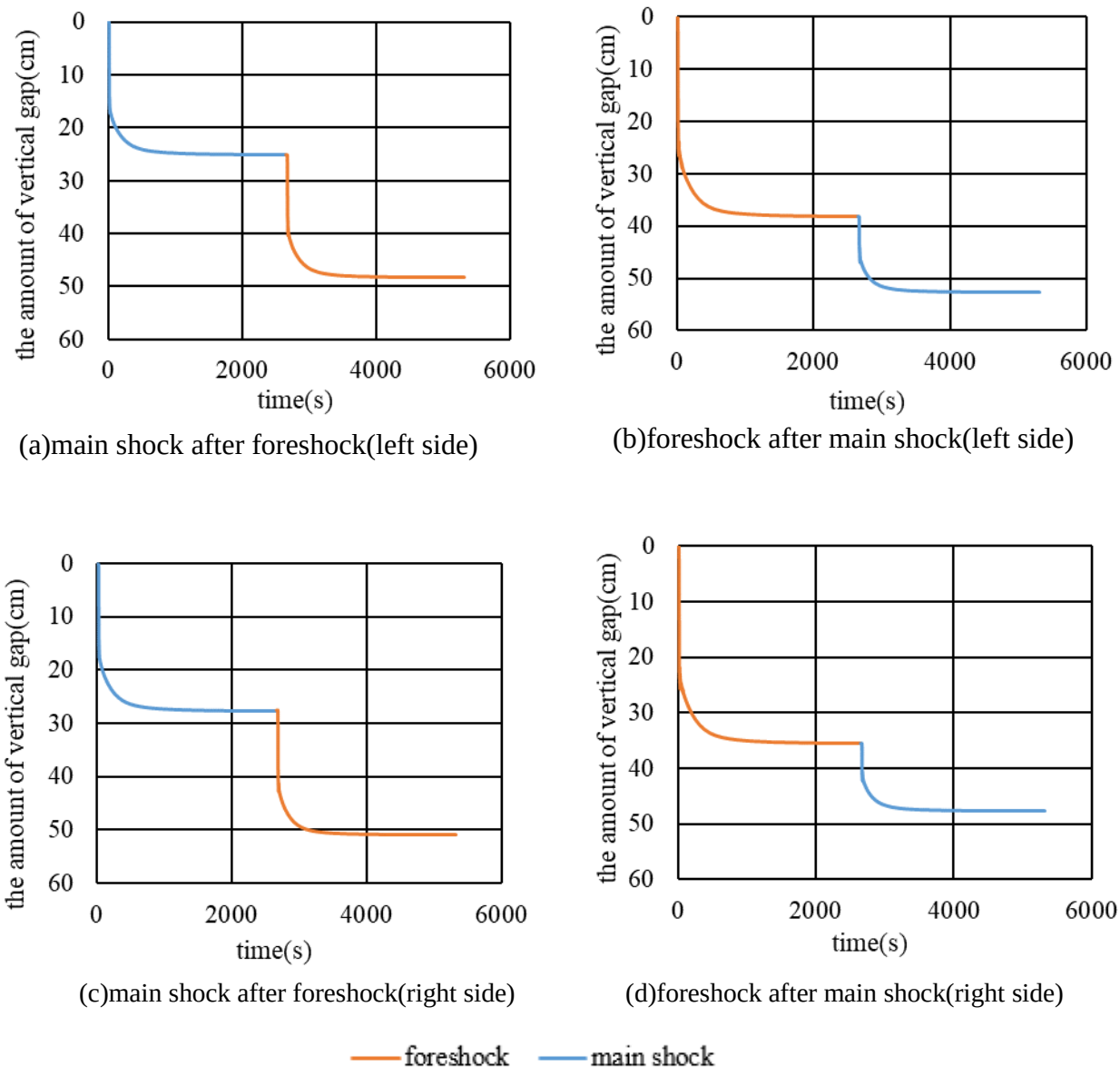

(a)main shock after foreshock(left side)

(b)foreshock after main shock(left side)

(c)main shock after foreshock(right side)

(d)foreshock after main shock(right side)

Fig. 7 - Time history of the amount of vertical gap (each section)

Table 2 and Table 3 show the convergence value after the first seismic motion and the second seismic motion, respectively. From Table 2 and Table 3, the final vertical gap is almost same (49.6cm and 50.1cm) even if the occurance order of two seismic motoin is changed. It is thought that tha total input energy is same. And the sum of the result of the model inputting fore shock and the model inputting main shock(26.1+36.9=63.0cm) is larger than the vertical gap of the model inputting fore shock and main shock (about 50cm) continuously. It is thought that the liquefaction layer compacted after the first seismic motion, so the amount of the subsidence is smaller when the second seismic motion is inputted.

Table-2 Amount of vetical gap (After the first seismic wave)

	foreshock	main shock
left side	25.0	38.2
right side	27.3	35.6
average	26.1	36.9

unit (cm)

Table-3 Amount of vetical gap (After the second seismic wave)

	main shock after foreshock	foreshock after main shock
left side	48.2	52.6
right side	51.0	47.7
average	49.6	50.1

unit (cm)

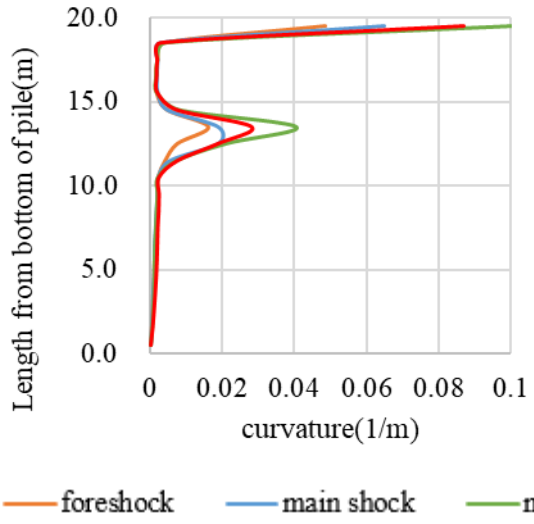

Fig. 8 - Maximum curvature

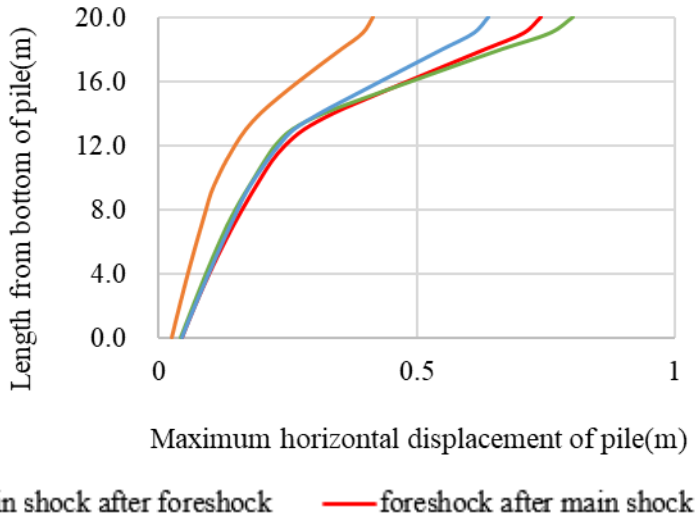

Fig. 9 - Maximum horizontal dispalacement

3.2 The response of pile foundation

Fig. 8 and Fig. 9 show the distribution of maximum curvature and maximum horizontal displacement of the pile at the center of the right abutment. The curvature and horizontal displacement are expressed as absolute values, and the yield curvature of the pile is 0.0017 (1/m). Fig. 8 shows that the largest curvature occurs at just below the foundation. This is because the bending moment becomes the largest value at the fixed end. The second largest (the second peak) curvature occurs at the height of about 13 m, that is at a little below the liquefaction layer. This is because the steel piles yielded at the height of about 10 m in this analysis. Then the curvature increases sharply. But the horizontal force acting from soil to the pile becomes smaller in the liquefaction layer due to the liquefaction. So, the second peak point is appeared at a little below the liquefaction layer. As mentioned before, in this analysis, the steel piles yielded by the first seismic motion. So, the maximum curvature and the displacement of the steel pile became larger by the second seismic motion. Same as the vertical gap, the maximum horizontal displacement of the pile is almost same even if the occurrence order of two seismic motion is changed.

4. CONCLUDING REMARKS

In this study, we focused on the subsidence phenomenon of the approaching area of the abutment when two strong motions, the foreshock on April 14, 2016 and the main shock on April 16, 2016, were input to a virtual bridge across the river. The results are obtained as follows,

(1) The final vertical gap is almost same even if the occurrence order of two seismic motion is changed. And the vertical gap of the model inputting fore shock and main shock continuously is smaller than the sum of the result of the model inputting fore shock and the model inputting main shock.

(2) The largest curvature occurs at just below the foundation. The second largest (the second peak) curvature occurs at a little below the liquefaction layer. This is because the horizontal force acting from soil to the pile becomes smaller in the liquefaction layer due to the liquefaction. The maximum curvature of the pile in the case that the foreshock and main shock are input consecutively is larger than the case of only the main shock. Same as the vertical gap, the maximum horizontal displacement of the pile is almost same even if the occurrence order of two seismic motion is changed.

Acknowledgement

This research was supported by JSPS KAKENHI Grant Number JP18K04332.

References

[1] Joint Editorial Committee for the Report on the Great East Japan Earthquake Disaster (2015): *Civil Engineering Part 1, Damages in Civil Engineering Structures from Earthquake and Restorations*, Japan Society of Civil Engineers, ISBN978-4-8106-0861-8 (in Japanese).

[2] Japan Society of Civil Engineers (2017): *Report on Damage Surveys and Investigations following the 2016 Kumamoto Earthquake*, ISBN978-4-8106-0951-6 (in Japanese).

[3] Iai, S., Matsunaga, Y., Kameoka, T. (1992): Analysis of Undrained Cyclic Behavior of Sand under Anisotropic Consolidation, *Soils and Foundations*, **32**(2), 16-20.

[4] Morita, T., Iai, S., Liu, H., Ichii, K., Sato, Y. (1997): Simplified Method to Determine Parameter of FLIP, *Technical Notes of the Port and Harbor Research Institute*, **869**, 1-36 (in Japanese).

[5] Strong-motion Seismograph Networks: http://www.kyoshin.bosai.go.jp/ (Accessed Feb.14, 2020).

